Button-Push On-Demand Synthesis for Rapid Optimization of Antiviral Peptidomimetics

Authors: Duanshuai Tian[1], Ting Wei Tan[1], Ronald Toh Kuan Hai[2], Gan Wang[1], Fadhil Peer Mohamed[1], Zhenyang Yu[1,3], Hwee Ting Ang[1], Weijun Xu[2], Qian Wen Tan[2], Pearly Ng[2], Choon Heng Low[2], Boping Liu[2], Perlyn Quek Zekui[2], Joma Kanikadu Joy[2], Joseph Cherian[2], Frankie Mak[2*], Jie Wu[1,3]*

Affiliations:

[1] Department of Chemistry, National University of Singapore, 3 Science Drive 3, 117543 Singapore

[2] Experimental Drug Development Centre, 10 Biopolis Rd, #05-01/06 Chromos, 138670 Singapore

[3] National University of Singapore (Chongqing) Research Institute, Chongqing, 401120, China

* Corresponding author. Email: frankie_mak@eddc.sg (F.M.); chmjie@nus.edu.sg (J.W.).

Abstract: Optimization of a lead compound into drug candidates is crucial in drug discovery, but often hampered by cumbersome manual synthesis of derivatives. While automated organic molecule synthesis has enhanced efficiency, safety, and cost-effectiveness, achieving fully automated multistep synthesis remains a formidable challenge due to issues like solvent and reagent incompatibilities and the accumulation of side-products. We herein demonstrate an automated solid-phase flow platform for synthesizing α-keto-amides and nitrile peptidomimetics, guided by docking simulations, to identify potent broad-spectrum antiviral leads. A compact parallel synthesizer was built in-house, which allows producing 5 distinct molecules per cycle. 525 reactions could be finished on this platform in three months to generate 42 derivatives, with eight exhibiting promising antiviral activity (IC_{50} < 100 nM). The platform, coupled with digital chemical recipe files, offers rapid access to a wide range of peptidomimetics, serving as a valuable reservoir for broad-spectrum antiviral candidates. This automated solid-phase flow synthesis approach expedites the generation of previously difficult complex molecular scaffolds, which has the potential to shift the paradigm of drug discovery, especially when combined with computer-aided drug design.

One-sentence summary: A parallel automated solid-phase flow synthesis platform was developed to accelerate the tructural optimization of peptidomimetics for the discovery of broad-spectrum antiviral agents.

Since the initial outbreak of the Severe Acute Respiratory Coronavirus (SARS-CoV-2) in early December 2019 (*1*), the world has witnessed over 690 million infections and nearly 7 million deaths (*2*). This relentless pandemic has profoundly challenged healthcare systems and global economies, while significantly altering daily lives (*3, 4*). The insights gained from this crisis are pivotal in reshaping the future of pharmaceutical development and public health strategy (*5*). It has underscored the critical need for a shift from conventional cumbersome and time-consuming drug discovery and development processes to more expeditious, streamlined approaches supported by innovative technologies (*6, 7*). Moreover, the establishment of a stockpile of broad-spectrum antiviral medications is crucial for quickly countering future viral outbreaks, enabling swift response and immediate availability of treatments (*8*).

Promising compounds in the context of viral inhibition include peptidomimetics featuring α-keto-amide or nitrile groups as functional warheads (*9-12*). These molecules are designed to mimic the natural substrates of viral proteases which are crucial for viral replication. The α-keto-amides and nitrile warheads form reversible covalent bond with viral proteases thereby disrupting viral replication leading to potent antiviral efficacy. Notable examples of α-keto-amide inhibitors include NS3 4A protease inhibitors such as boceprevir (*13, 14*) and telaprevir (*15, 16*), both employed in the treatment of Hepatitis C Virus (HCV) infections. Another example is the class of chymotrypsin-related protease (3Cpro) or 3CLpro inhibitors, like GC375 (*17*), exhibiting activity against a range of viruses including norovirus, SARS-CoV, and Hand-Foot-and-Mouth Disease (HFMD) Virus. Nitrile-based peptidomimetics also exhibit broad-spectrum inhibition against 3CLpro from various coronavirus strains (*18*). Of particular importance is paxlovid, a recently approved nitrile peptidomimetic, which has proven effective against SARS-CoV-2 (*19*) (Fig.1).

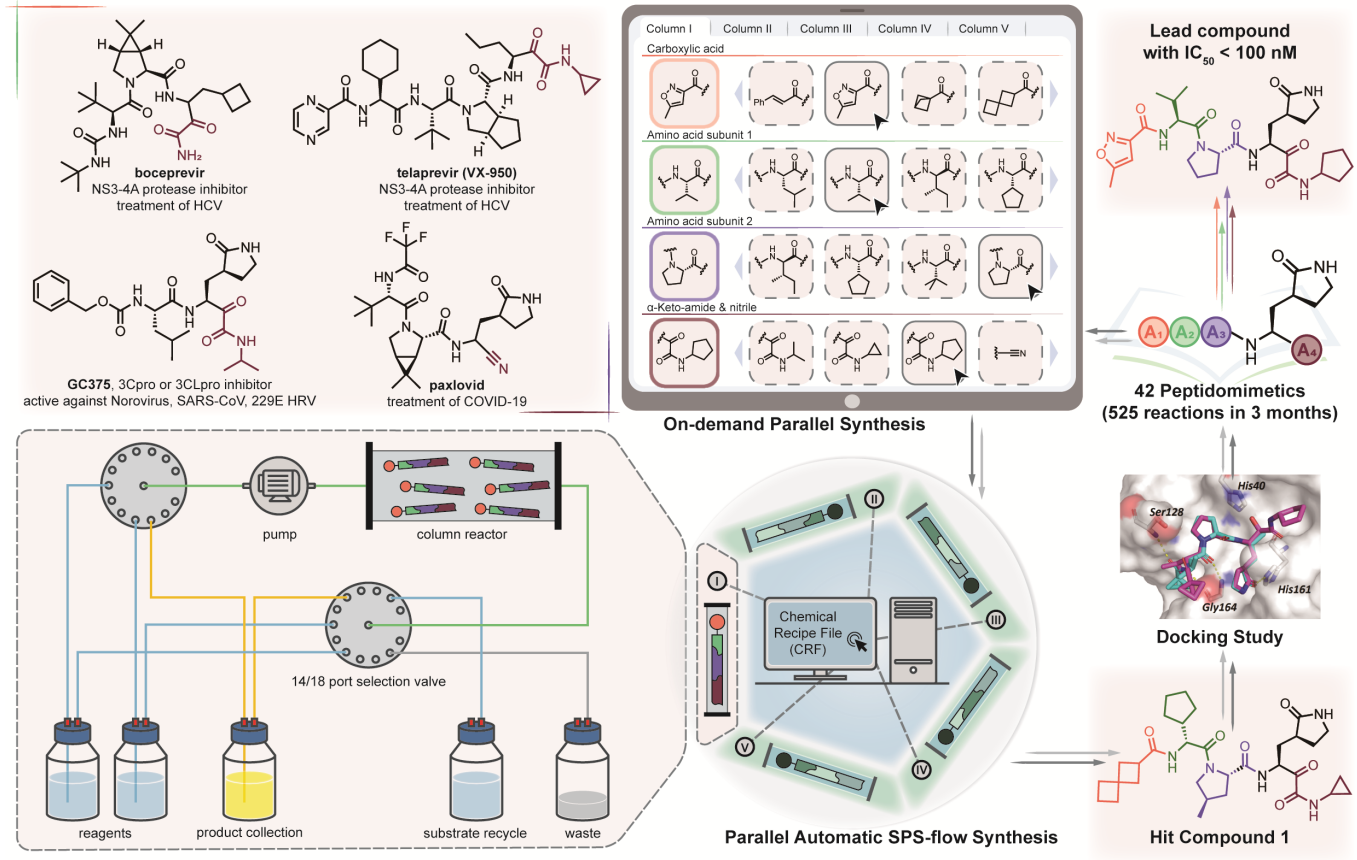


Fig. 1. Development of parallel automatic synthesis platform for the efficient synthesis of α-keto-amides and nitrile peptidomimetics with potent antiviral activity.

While α-keto-amides and nitrile peptidomimetics hold significant potential as broad-spectrum

antiviral agents, further investigations are needed to fully explore and optimize their therapeutic potential considering the variability in the residues lining the binding pocket of the catalytic site of different viral proteases. Currently, the synthesis of these compounds predominantly relies on conventional batch solution-phase synthesis methods (*20*). The inherent complexity of these compounds often leads to lengthy synthesis procedures with cumbersome post-purification campaign, largely limiting the synthetic efficiency and generating substantial waste. These challenges highlight the urgent need for innovative synthetic technologies that can enhance efficiency and reduce waste generation. While transitioning from conventional batch solution-phase synthesis to automated pharmaceutical molecule assembly (*21-26*) is a promising solution, achieving fully automated multistep synthesis remains a formidable challenge. Issues such as incompatibility between different reaction steps, the accumulation of side-products, as well as the difficulties of implementing reliable automation systems capable of handling diverse reactions and reagents need to be overcome.

SPS-flow synthesis, a powerful amalgamation of solid-phase synthesis (SPS) — renowned for its widespread applications in the automated synthesis of peptides and oligonucleotides (*27, 28*) — and flow reactor technology — increasingly recognized as an excellent tool for the automated synthesis of small molecule drugs (*29*) — presents a streamlined approach to automated multistep synthesis. The ease of purification between each step, facilitated by simple solvent washing in SPS, adeptly minimizes by-product accumulation. This cohesive process not only enables efficient impurity removal but also effectively addresses challenges associated with the compatibility between multiple reaction steps. On the other hand, the seamless integration with control systems, including pumps and valves, the flow system enhances the overall efficiency of SPS-flow synthesis, offering a convenient, efficient, and universally applicable methodology. This integration holds the promise of synergistically enhancing streamlined automation with broader reaction patterns and longer synthetic sequences. The Pentelute group has demonstrated the successful application of SPS-flow technology in the automated synthesis of peptides, proteins (*30*), and oligonucleotide mimetics (*31*). Recently, our group showcased the efficacy of this technology through a button-push, automated six-step synthesis of perxasertib and its derivatives (*32*). The established Chemical Recipe File (CRF) can be seamlessly adapted for on-demand automated synthesis of derivatives by strategically altering the starting building blocks at any step of the synthesis.

In contrast to traditional batch solution-phase synthesis, the SPS-flow platform demonstrates particular suitability for peptidomimetic synthesis, significantly reducing both time and manpower involvement by eliminating the need for laborious post-purification after each synthetic step. Moving forward, we anticipate that integration of SPS-flow technology with parallel synthesis and computer-aided drug design for the peptidomimetics synthesis holds the potential to significantly increase the chances of identifying effective drug candidates. This approach promises to expedite the lead optimization process, offering a time-efficient and resource-saving alternative to conventional resource-intensive combinatorial synthesis for chemical space exploration. The established digital CRF provides the capability to directly generate any desired peptidomimetic compounds within the defined scaffold scope in a button-push fashion. These capabilities position this integrated platform as a valuable reservoir of candidate compounds for broad-spectrum antiviral agents, strategically prepared to address future pandemic challenges.

We herein report the successful implementation of SPS-flow technology for automated parallel on-demand synthesis of α-keto-amide and nitrile peptidomimetics guided by computational docking simulations, accelerating the hit-to-lead campaign for broad spectrum antiviral therapies (Fig.1). Our in-house-built compact synthesis platform, featuring five column reactors, facilitated the simultaneous production of five distinct target compounds in a single run, enabling the synthesis of 42 derivatives on this automated platform within 3 months, with eight compounds exhibited notable inhibitory activity (IC_{50} values below 100 nM) against 3Cpro in both Enteroviruses (EV) and Human Rhinovirus (HRV). Additionally, the same platform, along with the established CRF, is readily applicable for scaling up the synthesis of potential lead compounds to several hundred milligrams for *in-vivo* pharmacokinetics and pharmacology studies.

Targeted peptidomimetics identification. EV and HRV infections are increasingly associated with severe outcomes, including neurological complications and fatalities, capturing the attention of the public and medical researchers (*33*). However, there remains a lack of approved antiviral therapies targeting these viruses, highlighting an urgent need for broad-spectrum antiviral compounds that target conserved elements essential for viral replication. In this case, our study started with identifying inhibitors of 3Cpro in EV and HRV. The 3Cpro enzyme is critical for proteolytic cleavage, transforming large proteins into functional proteins and enzymes essential for viral replication (*34*). In our recent investigations into novel inhibitors of the SARS-CoV-2 3CL protease, we discovered that compound **1** effectively inhibited HRV 3Cpro, albeit limited inhibitory activity against the SARS-CoV-2 3CLpro. To explore the potential of compound **1** for broad-spectrum antiviral agents targeting 3Cpro, we performed a structural alignment and comparison based on a 3D superimposition of the active sites of 3C proteases across HRV, Coxsackie (COX)-B3, EV68 and EV71. Using the rupintrivir-bound EV68 co-crystal structure as a reference (pdb: 7L8H), we observed a high degree of similarity in the amino acids surrounding the ligand (fig. S17). Armed with these insights, we embarked on a hit-to-lead campaign for compound **1**. The targeted compound structures include one carboxylic acid, two amino acids, and one α-keto-amide subunit, providing four variables for generating various derivatives in the hit-to-lead campaign. Additionally, although compound **1** is a α-keto-amide peptidomimetic, we leveraged the capabilities of the SPS-flow platform to explore compounds containing alternate warheads such as a nitrile group as a subseries.

Generation of digital chemical recipe files (CRFs) for the SPS-flow synthesis of α-keto-amide and nitrile peptidomimetics. The key to the success of automated SPS-flow synthesis lies in the rapid generation of robust and general CRFs. Despite the seemingly straightforward assembly of the scaffolds in compound **1**, we faced multiple challenges in establishing the CRFs. The first obstacle arises from the low reactivity of the amide functional groups in the targeted scaffolds, complicating the attachment of starting materials to the solid resin. Additionally, the presence of several chiral centers in the scaffolds requires cautious synthetic conditions to prevent racemization.

Our study began with the development of an effective protocol for attaching the starting material to a solid resin and the subsequent convenient cleavage of the final product from the resin matrix (fig. S1). Notably, lactam **S-2** underwent an S_N1 reaction with a diaryl alcohol in acetic acid to form compound **S-3** while preserving the chiral stereocenters. In the cleavage step, the C–N bond could be efficiently cleaved in TFA/DCM (1:1) without affecting the labile keto-amide functional group. These results suggested that using this approach to bind the initial lactam to a solid resin containing a diaryl alcohol linker and cleave the final product from the resin is feasibility. Thereafter, to achieve the optimal reaction conditions for SPS, we established a 13-step synthetic protocol for batch solution-phase synthesis of the model α-keto-amide compound **2**, achieving an overall yield of 18% (fig. S4). However, the post-reaction treatment is cumbersome, requiring a total of 10 rounds of column chromatography for purification. Noteworthily, all synthetic procedures were conducted at ambient conditions, which helps to suppress the epimerization of chiral centers and simplifies the subsequent setup of the SPS-flow system.

To transform the batch solution-phase synthesis into SPS-flow synthesis, we modified Wang resin by introducing a diaryl alcohol linker, which was used as the solid matrix for the subsequent study (fig. S3). Gratiftingly, the pre-established conditions in batch solution-phase synthesis could be directly adapted to SPS-flow synthesis by incorporating simple solvent washing steps in between each step. It is worth noting that the remarkable solvent cleaning efficiency enables strategic use of excess reagents to ensure high yields (fig. S7 and table S1). Significantly, the SPS-flow synthesis, comprising 13 steps, required only a single post-purification step following the final cleavage, where the crude reaction mixture was purified with preparative thin-layer chromatography (prep-TLC) to afford the pure target product **2** (107 mg from 1 g of resin) with an improved overall yield of 35%. Moreover, the entire process required only 2.5 liters of solvent, marking a substantial reduction compared to that used in the batch solution-phase synthesis protocol. With the SPS-flow protocol established for compound **2**, a CRF was easily established for synthesizing α-keto-amide peptidomimetic derivatives (Fig. 2A).

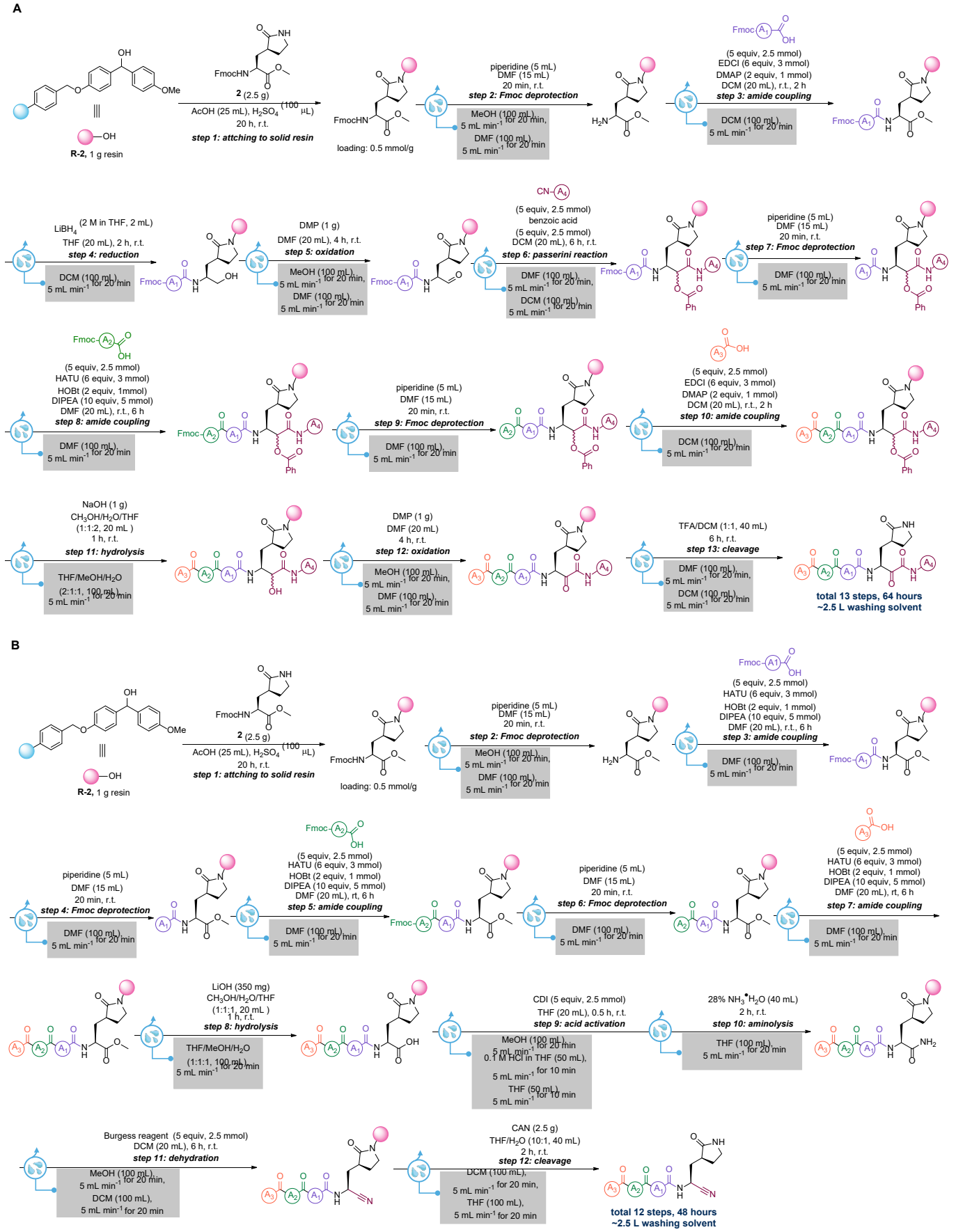


Fig. 2. Schematic scheme of the established CRFs for the synthesis of *α*-keto-amide and nitrile compounds. (**A**) CRF for the synthesis of *α*-keto-amides. (**B**) CRF for the synthesis of nitrile compounds. Loading of the first step was confirmed by analysis of ^{1}H NMR spectrum of the cleaved compound with

1,3,5-trimethoxybenzene as an internal standard. DMF, dimethylformamide; THF, tetrahydrofuran; DCM, dichloromethane; TFA, trifluoroacetic acid; EDCI, 1-ethyl-3-(3-dimethylaminopropyl) carbodiimide; HATU, hexafluorophosphate azabenzotriazole tetramethyl uronium; DMAP, 4-dimethylaminopyridine; DMP, Dess–Martin periodinane; HOBt, 1-hydroxybenzotriazole; r.t., room temperature; DIPEA, N,N-diisopropylethylamine; CDI, 1,1'-carbonyldiimidazole; CAN, ceric ammonium nitrate.

Additionally, we successfully developed a CRF for the nitrile compounds without resorting to batch solution-phase synthesis by modifying the SPS-flow synthesis protocol of keto-amide **2**. Although the cleavage of nitrile peptidomimetics from the solid presented a unique challenge due to the instability of the nitrile group under acidic conditions, it was successfully addressed by employing oxidative cleavage ceric ammonium nitrate (CAN) as the oxidant (Fig. 2B, fig. S9 and table S2).

Establishment of the parallel automated synthesizer. To further enhance the efficiency of the synthesis process and enable on-demand button-push synthesis, an automated SPS-flow synthesizer featuring five parallel column reactors was established (Fig. 3). The system is comprised of five milligat pumps, ten multiway selection valves, five perfluoroalkoxy (PFA) column reactors (each equipped with frits featuring 200 mesh pores; fig. S6), and a Python-interfaced computer system (fig. S11). The synthetic protocol was digitally encoded using Python programming, outlining the process modules, fluid paths, stock solution and solvent locations, and flow rates. Based on the codes, the computer system manages the seamless coordination of all units, ensuring efficient transfer of reagents and solvents from designated stock locations to the column reactors. This process facilitates the digital storage of the CRF for implementation on-demand.

This custom-built platform is remarkably compact and can be fitted within a standard fume hood (70 cm width×150 cm length×90 cm height). The working process of this platform was showcased in the Supplementary Video. With this system, five distinct target compounds could be prepared within four days, each requiring only a single final purification, underscoring a significant improvment in efficiency and a substantial reduction in labor and resource expenditure compared to traditional batch solution-phase synthesis methods. In total, 525 reactions were thus operated within 3 months to afford 21 α-keto-amide and 21 nitrile peptidomimetics in moderate to good yields (fig. S14).

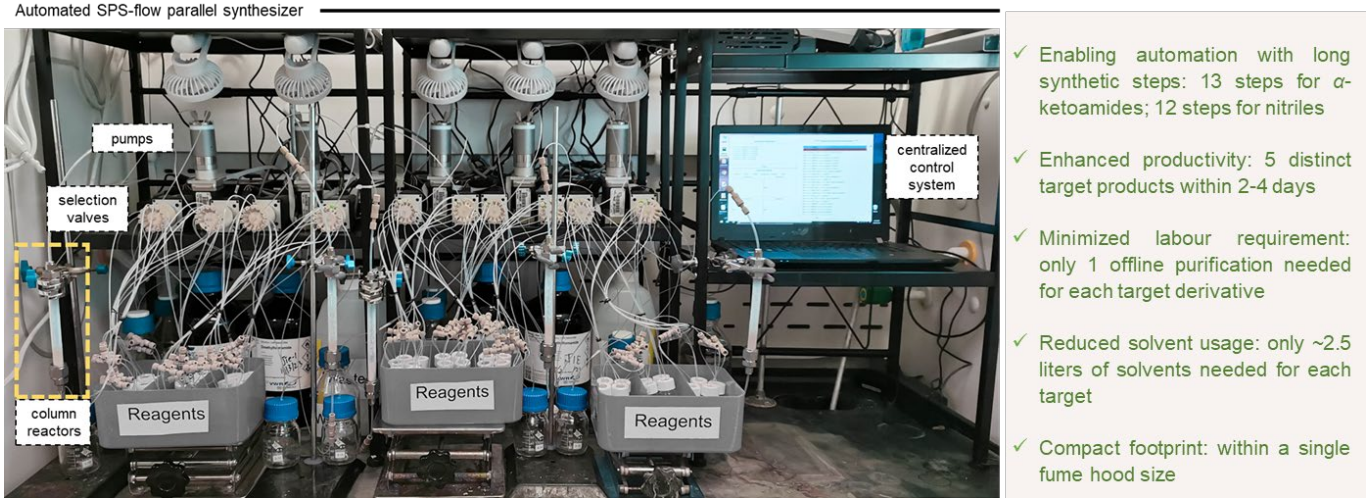
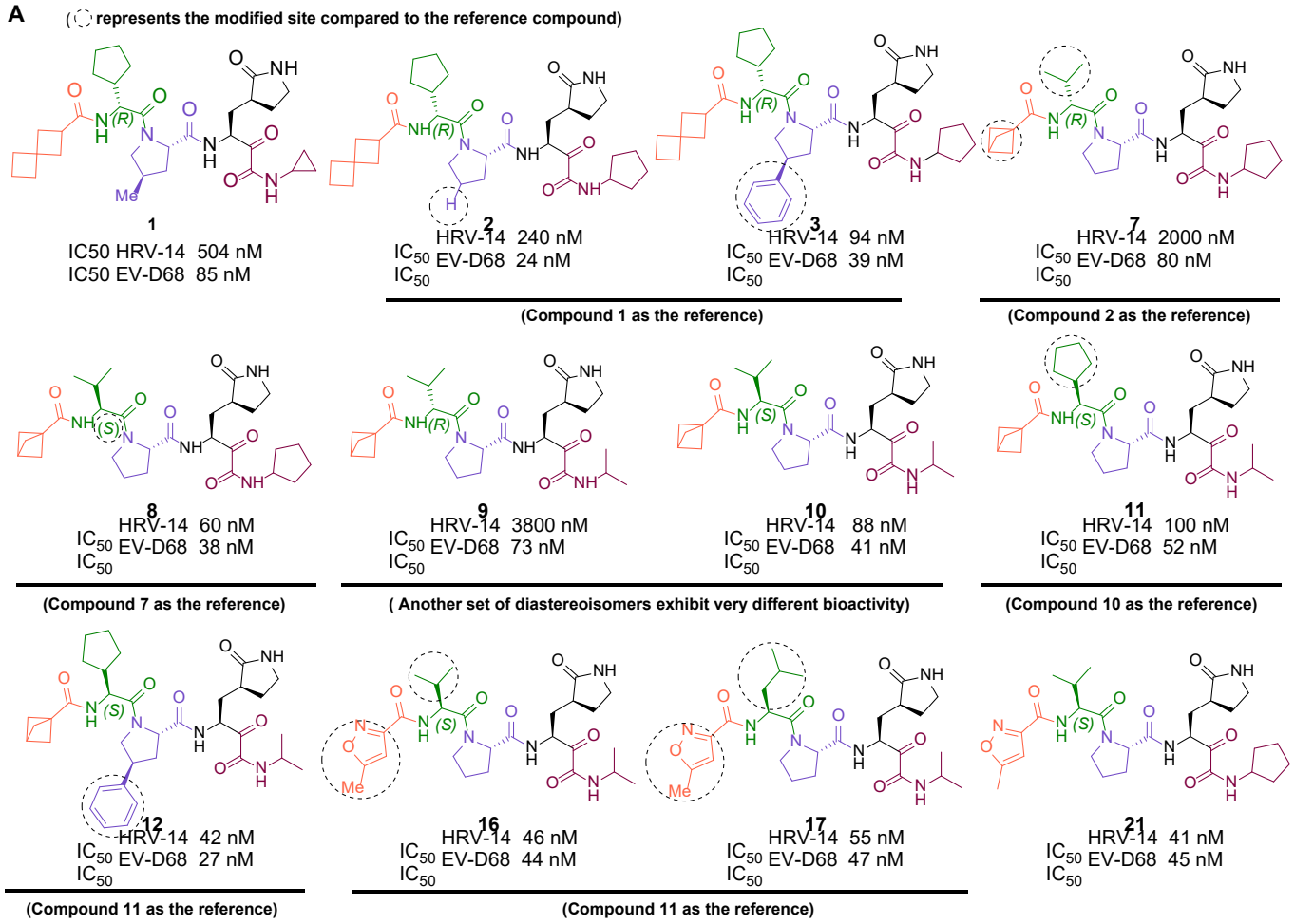
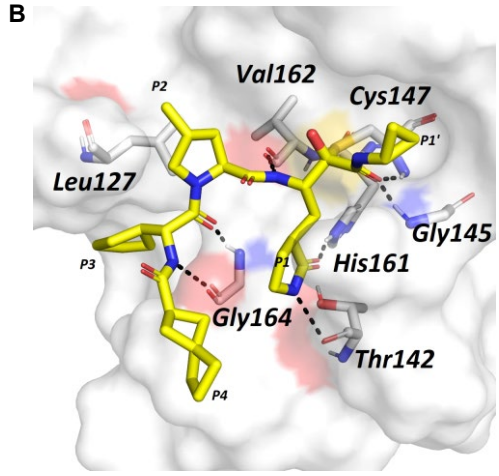


Fig. 3. Setup of the SPS-flow parallel synthesizer. For reagent/solvent-port connections, see fig. S11C.

SAR exploration.

Given the promising inhibitory activity of compound **1** against the EV 3C protease (85 nM), our medicinal chemistry efforts pivoted towards identifying a lead compound with improved efficacy against the HRV 3C protease (Fig. 4A). Docking of compound **1** with the crystal structure of HRV 3C protease suggested potential lipophilic interaction within the P2 pocket for potency gain (Fig. 4B). Comparative bioactivity assessments revealed that α-keto-amide peptidomimetics outperformed nitrile peptidomimetics





C

	Compound 3	Compound 21
Measured LogD pH 7.4	4.7	1.0
Thermodynamic solubility pH 7.4 (μg/mL)	110.3	979.4
PAMPA Pe 10-6 (cm/sec)	38.08	0.18
Cl_{int} HLM, RLM (μL/min/mg)	142, 62	0, 1
Plasma Stability H, R ($T_{1/2}$ - min)	>240	>240
PPB H, R (% unbound)	1.76, 0.64	50.7, 45.4

Fig. 4. SAR exploration. (**A**) IC_{50} values of selected compounds against HRV-14 and EV-D68 3C protease. (**B**) The docked pose of compound **1** with crystal structure of HRV 3C protease (PDB code: 5XF6). The 5-membered lactam formed H-bond interactions with Thr142 and His161; amide oxygen of the ketoamide warhead interacted with the backbone NH group of both Gly145 and Cys147; NH of the amide bond between P2 proline and P1 glutamine made a H-bond contact with the backbone carbonyl oxygen of Val162 while the NH of P3 amino acid residue formed H-bond interaction with the backbone carbonyl oxygen from Gly164. The cyclopropyl moiety of the ketoamide warhead was surrounded by hydrophobic residues and likely formed beneficial van der Waal interactions. (**C**) *In vitro* ADME profile of compounds **3** and **21**. PAMPA: Parallel Artificial Membrane Permeability Assay; Cl_{int} HLM, RLM: intrinsic clearance Human Liver Microsomes, Rat Liver Microsomes; PPB H, R: Plasma Protein Binding Human, Rat.

in target inhibitory activity (fig. S20). From 21 synthesized α-keto-amide peptidomimetics, 12 representative compounds were selected for detailed analysis to elucidate key structure-activity relationships (SAR). Replacing the methyl group in compound **1** with hydrogen and phenyl substituent showed only marginal improvement in potency (**2** and **3**). Moreover, *in-vitro* ADME (absorption, distribution, metabolism and excretion) profiling of **3** revealed the highly protein bound (>98%), high microsomal and high permeability profile (Fig. 4C). On the other hand, reducing the size of cyclopentyl and spiro [3.3] heptyl in compound **2** to modulate lipophilicity resulted in significantly reduced potency (**7** – 2000 nM). Interestingly, the *S*-diastereomer of compound **7** was significantly more potent (**8** – 60 nM). This observation was further supported by testing another diastereomeric pair, where the *S*-diastereomer (**10** – 88 nM) was again significantly more potent than its *R*-diastereomer (**9** – 3800 nM). The observed increase in potency could be attributed to the specific interactions between Ser128 and Gly164 residues and the terminal peptide associated with *S*-configuration (fig. S18). Notably, a close analogue to compound **10** with a cyclopentyl of *S*-configuration (**11**) resulted in no potency improvement and exploration of the P2 pocket in **12** with a phenyl substituent also showed similar potency. Subsequent efforts to replace bicyclo[1.1.1]pentyl group in compound **11** with a methyl isoxazole group and substituting cyclopentyl group with isopropyl or isobutyl group to increase conformational flexibility (**16** and **17**) did not lead to significant potency improvement. However, a closely related analogue (**21**) demonstrated good potency and an improved *in-vitro* ADME profile compared to compound **3** (Fig. 4C). Based on the hit compound **1,** it is encouraging to identify a compound (**21**) with more than ten-fold potency improvement and a decent *in-vitro* ADME profile from a small set of analogues, which will guide the next phase of optimization leveraging our parallel automatic SPS-flow synthesis platform in a resource- and time-efficient manner.

Scaling up synthesis. With compound **21** identified as the lead from this set of analogues, a larger amount of compound **21** is needed for upcoming *in vivo* pharmacokinetics and pharmacology studies. Through the established system with the CRF, we could directly synthesize over 350 mg of compound **21** by running the parallel reactors in one cycle using the automated synthesizer.

Conclusion and outlook. We have successfully established a SPS-flow parallel automatic synthesis platform that conveniently fits within a 1.5-meter-long fume hood. This platform encompasses five column reactors, enabling the simultaneous production of five distinct target products in a single operational cycle. This technological advancement significantly accelerates the lead optimization process by facilitating direct access to specifically designed derivatives for SAR studies within a short timeframe. Two general CRFs were generated, leading to the synthesis of 21 α-keto-amides and 21 nitrile peptidomimetics within three months in a streamlined, button-push, on-demand fashion. The digitalized CRFs enable the rapid generation of targeted peptidomimetics by modifying any specific amino-acid fragments, thereby positioning these CRFs as a valuable reservoir of broad-spectrum antiviral agents. Notably, eight out of the 42 synthesized compounds exhibited good bioactivity, exhibiting IC_{50} values of HRV-14 protease below 100 nM. Additionally, the platform was directly applied to produce over 350 milligrams of compound **21** for future *in vivo* pharmacokinetics and pharmacology studies.

In conclusion, our platform has demonstrated its potential in establishing of an extensive reservoir of peptidomimetics, thereby positioning itself as a pivotal tool for biochemists to facilitate the comprehensive investigation of the potential applications of these compounds in antiviral drug research. This study also underscores the profound impact of integrating SPS-flow synthesis technology with medicinal chemistry-guided optimization, which has the potential to revolutionize drug discovery processes in pharmaceutical endeavors. Hence, our methodology represents a significant step forward in refining strategies to enhance human preparedness and response to future viral disease outbreaks.

References and Notes

1. A. K. Sharma, Novel Coronavirus Disease (COVID-19). *Resonance* **25**, 647-668 (2020).

2. https://www.worldometers.info/coronavirus/.
3. T. Dong *et al.*, Sensitive Lateral Flow Immunoassay Based on Specific Peptide and Superior Oxidase Mimics with a Universal Dual-Mode Significant Signal Amplification. *Anal. Chem.* **95**, 12532-12540 (2023).
4. K. E. Ukhurebor, K. R. Singh, V. Nayak, G. Uk-Eghonghon, Influence of the SARS-CoV-2 pandemic: a review from the climate change perspective. *Environ. Sci. Process. Impacts.* **23**, 1060-1078 (2021).
5. N. Ayati, P. Saiyarsarai, S. Nikfar, Short and long term impacts of COVID-19 on the pharmaceutical sector. *Daru.* **28**, 799-805 (2020).
6. M. Yadav, S. Dhagat, J. S. Eswari, Emerging strategies on in silico drug development against COVID-19: challenges and opportunities. *Eur. J. Pharm. Sci.* **155**, 105522 (2020).
7. E. N. Muratov *et al.*, A critical overview of computational approaches employed for COVID-19 drug discovery. *Chem. Soc. Rev.* **50**, 9121-9151 (2021).
8. D. van Riel, E. de Wit, Next-generation vaccine platforms for COVID-19. *Nat. Mater.* **19**, 810-812 (2020).
9. L. Zhang *et al.*, Crystal structure of SARS-CoV-2 main protease provides a basis for design of improved α-ketoamide inhibitors. *Science* **368**, 409-412 (2020).
10. L. Zhang *et al.*, alpha-Ketoamides as Broad-Spectrum Inhibitors of Coronavirus and Enterovirus Replication: Structure-Based Design, Synthesis, and Activity Assessment. *J. Med. Chem.* **63**, 4562-4578 (2020).
11. J. Zhou, A. Saha, Z. Huang, A. Warshel, Fast and Effective Prediction of the Absolute Binding Free Energies of Covalent Inhibitors of SARS-CoV-2 Main Protease and 20S Proteasome. *J. Am. Chem. Soc.* **144**, 7568-7572 (2022).
12. M. Robello *et al.*, The Alpha Keto Amide Moiety as a Privileged Motif in Medicinal Chemistry: Current Insights and Emerging Opportunities. *J. Med. Chem.* **64**, 3508-3545 (2021).
13. F. G. Njoroge, K. X. Chen, N.-Y. Shih, J. J. Piwinski, Challenges in Modern Drug Discovery: A Case Study of Boceprevir, an HCV Protease Inhibitor for the Treatment of Hepatitis C Virus Infection. *Acc. Chem. Res.* **41**, 50-59 (2008).
14. F. Poordad *et al.*, Boceprevir for untreated chronic HCV genotype 1 infection. *N. Engl. J. Med.* **364**, 1195-1206 (2011).
15. A. D. Kwong, R. S. Kauffman, P. Hurter, P. Mueller, Discovery and development of telaprevir: an NS3-4A protease inhibitor for treating genotype 1 chronic hepatitis C virus. *Nat. Biotechnol.* **29**, 993-1003 (2011).
16. F. Guillier, D. Orain, M. Bradley, Linkers and Cleavage Strategies in Solid-Phase Organic Synthesis and Combinatorial Chemistry. *Chem. Rev.* **100**, 2091-2158 (2000).
17. Y. Kim *et al.*, Broad-spectrum antivirals against 3C or 3C-like proteases of picornaviruses, noroviruses, and coronaviruses. *J. Virol.* **86**, 11754-11762 (2012).
18. C. P. Chuck *et al.*, Design, synthesis and crystallographic analysis of nitrile-based broad-spectrum peptidomimetic inhibitors for coronavirus 3C-like proteases. *Eur. J. Med. Chem.* **59**, 1-6 (2013).
19. D. R. Owen *et al.*, An oral SARS-CoV-2 M(pro) inhibitor clinical candidate for the treatment of COVID-19. *Science* **374**, 1586-1593 (2021).
20. C. De Risi, G. P. Pollini, V. Zanirato, Recent Developments in General Methodologies for the Synthesis of alpha-Ketoamides. *Chem. Rev.* **116**, 3241-3305 (2016).
21. G. Wang, H. T. Ang, S. R. Dubbaka, P. O'Neill, J. Wu, Multistep automated synthesis of pharmaceuticals. *Trends. Chem.* **5**, 432-445 (2023).
22. M. Trobe, M. D. Burke, The Molecular Industrial Revolution: Automated Synthesis of Small Molecules. *Angew. Chem. Int. Ed.* **57**, 4192-4214 (2018).
23. S. V. Ley, D. E. Fitzpatrick, R. J. Ingham, R. M. Myers, Organic synthesis: march of the machines. *Angew. Chem. Int. Ed.* **54**, 3449-3464 (2015).
24. D. J. Blair *et al.*, Automated iterative Csp3–C bond formation. *Nature* **604**, 92-97 (2022).
25. J. Li *et al.*, Synthesis of many different types of organic small molecules using one automated process. *Science* **347**, 1221-1226 (2015).

26. S. Steiner *et al.*, Organic synthesis in a modular robotic system driven by a chemical programming language. *Science* **363**, eaav2211 (2019).
27. R. B. Merrifield, Automated Synthesis of Peptides. *Science* **150**, 178-185 (1965).
28. P. H. Seeberger, Automated carbohydrate synthesis to drive chemical glycomics. *Chem. Commun*. 1115-1121 (2003).
29. C. P. Breen, A. M. K. Nambiar, T. F. Jamison, K. F. Jensen, Ready, Set, Flow! Automated Continuous Synthesis and Optimization. *Trends. Chem.* **3**, 373-386 (2021).
30. N. Hartrampf *et al.*, Synthesis of proteins by automated flow chemistry. *Science* **368**, 980-987 (2020).
31. C. Li *et al.*, Fully automated fast-flow synthesis of antisense phosphorodiamidate morpholino oligomers. *Nat. Commun.* **12**, 4396 (2021).
32. C. Liu *et al.*, Automated synthesis of prexasertib and derivatives enabled by continuous-flow solid-phase synthesis. *Nat. Chem.* **13**, 451-457 (2021).
33. L. Royston, C. Tapparel, Rhinoviruses and Respiratory Enteroviruses: Not as Simple as ABC. *Viruses* **8**, (2016).
34. D. Sun, S. Chen, A. Cheng, M. Wang, Roles of the Picornaviral 3C Proteinase in the Viral Life Cycle and Host Cells. *Viruses* **8**, 82 (2016).

ACKNOWLEDGMENTS

Data availability: All data are available in the main text or the supplementary materials.

Code availability: The Python code for operating the SPS-flow automated synthesis in this study is available at https://github.com/tian-auto/automatic-SPS-Flow-synthesis-of--keto-amide-and-nitrile-peptidomimetics-.git

Funding: We are grateful for the financial support provided by National Research Foundation, the Prime Minister's Office of Singapore under its NRF-CRP Programme (award no. NRF-CRP25-2020RS-0002).

Author contributions

J.W., F.M., J.C., P.N., C.H.L. and T.Q.W. conceived and designed the experiments. D.T., T.W.T., R.T.K.H., F.P.M., Z.Y., B.L. and P.Q.Z performed the experiments. J.W., D.T., T.W.T., J.C. and F.M. analysed the experimental data. D.T. built the SPS-flow reactor system. D.T. and T.W.T. performed the Python programming for automated control. W.X. performed the molecular modelling studies. J.K.J. designed construct for EV-D68 soluble protein. J.W., J.C., F.M., D.T., G.W. wrote the manuscript with input from all authors. J.W. guided the project. All of the authors have approved the final version of the manuscript. We thank Siew Pheng Lim for her contributions to the 3Cpro protease inhibitor project.

Competing interests
The authors declare no competing interests.

Supplementary Materials

Materials and Methods

Supplementary Text

Figs. S1 to S69

Tables S1 to S4

References (*35-37*)

Supplementary Video